The International Journal of Materials and Engineering Technology (TIJMET) (2023) 6(2)
http://dergipark.gov.tr/tijmet
ISSN: 2667-4033

RESEARCH ARTICLE

Investigation of compatibility of AL5182 series sheets with DP800 series sheets by CMT method

Cihan Yakupoğlu[*1], Ufuk Öztürk[1], İbrahim Acar[2] and Faruk Varol[2]

[1]*Akpres Metal Yedek Parça Mak. San. Ve Tic. A.Ş, Centre of Research & Development, Sakarya, Türkiye*
[2]*Sakarya University of Applied Sciences University, Vocational School of Karasu, Sakarya, Türkiye*

Article Info

Article history:
Received 09.12.2023
Revised: 21.12.2023
Accepted: 26.12.2023
Published Online: 31.12.2023

Keywords:
DP800 steel
Al5182
Cold metal transfer
ER4043

Abstract

In this study, 1 mm thick DP800 (Double Phase) galvanized coated steel sheets used in the production of automotive body and chassis parts were combined with 1.5 mm thick Al 5182 series sheets. These connections were made using the cold metal transfer (CMT) method of gas arc welding. The applied welding position is determined as the overlap. This application was carried out in a fully automatic robotic system using 1 mm diameter aluminum-based ER4043 (AlSi5) filling wire. After joining processes with the cold metal transfer (CMT) method, tensile strength (MPa), bending test, hardness values (HV), macro and micro tests in the joining areas were examined. In conclusion, the maximum breaking strength was reached at 90 amps (Fm: 4.28 kN). It was observed that heat input affected the intermetallic (IMC) phase formation and thickness. In bending tests, the highest breaking force (295 N) was reached at 85 amperes. Negative effects of evaporative galvanization (incomplete melting, pore formation) were observed in Al-DP steel joints. It was observed that the melting of aluminum positively affected the wetting angle in galvanization.

1. Introduction

Weight reduction in the automotive sector is of great importance for the goals of reducing fuel consumption and CO2 emissions. Therefore, the use of unalloyed and ultra-high strength steels for durability has greatly increased. Non-ferrous light metal alloys and Al alloys are used in vehicle production due to their strength-to-weight ratio. Different materials such as steel and Al alloys are present in vehicle body structures, but the welded joining process of these different materials is of great importance. CMT (cold metal transfer), waveform controlled cold arc, pulsed double electrode gas arc and AC pulsed gas arc welding methods have been developed for the welding of thin sheet metal parts. These developed methods have been investigated in the application of joining different metals such as aluminum and steel. in many cases, galvanized steel has been used as steel base material [1-4]. The steel sheet has a Zn coating layer to prevent oxidation. In the case of hard-seam welding, the Zn in the Zn-coated material used may remain outside the joint. In recent studies, uncoated steel or aluminized steel [5-8] has been preferred over Zn-coated steel for joining dissimilar metals. In uncoated steels, the joining process is not suitable due to insufficient wetting due to oxidation. Babu et al. (2018) studied the feasibility of joining aluminum alloy (AA 2219) with austenitic stainless steel (AISI 321) in an overlap configuration was investigated using a hybrid fabrication route consisting of friction surfacing and cold metal transfer (CMT) welding. Friction surfacing of aluminum on stainless steel followed by CMT welding was found to be a promising approach for joining aluminum with stainless steel in overlap configuration [9]. Madhavan et al. (2016) studied the to join A6061-T6 aluminum alloy to Dual Phase 800 steel using AlSiMn filler by cold metal transfer (CMT) processes. Revealed the presence of elongated plate shape (Al5FeSi) and fragmented particles in the IM layer, found that welding currents and arc length correction factor have significant effects on joint strength and that tensile rupture occurs in the heat affected zone [10]. Singh et al. (2020) studied the new CMT+P brazing process was used to join aluminum (AA5052) and steel (DP780) in the lap position with increasing Al sheet thickness and found that the wettability and strength of CMT brazed joints decreased due to the gradual decrease in interfacial area with increasing Al thickness due to faster heat dissipation from molten filler [11].

In this study, the mechanical strength values and bending forces of the joints were determined by CMT joining method using a 1 mm diameter weld zone in the lap joint of 1 mm thick DP800 (Dual Phase) steel sheet and 1.5 mm thick Al 5182 sheet. ER4043 (AlSi5) filler wire was used. Hardness values in the weld zone were observed with varying welding current, the thickness of the formation of intermetallic structures of alloying elements (Al-FE-Si etc.) with heat and the effect of this formation and thickness on strength, the effect of zinc layer on wettability in the weld pool and structural properties in the joint with different amperage values (75A, 80A, 85A, 90A, 95A, 100A, 105A) were observed.

2. Materials and methods

2.1. Materials used in the experiments

DP800 galvanized steel and Al 5182 sheet were used as test materials in the experiments. The steel sheet is 1 mm thick and 12-14 micron (45-60 g/m2) galvanized on both surfaces. Al 5182 (AL5- HDI-TZ-U) sheet metal was chosen with a

Corresponding Author: Cihan Yakupoğlu
E-mail: cihan.yakupoglu@akpres.com.tr

How to cite this article:
Yakupoğlu, C., Öztürk, U., Acar, İ.,Varol, F., Investigation of Compatibility of Al5182 Series Sheets with DP800 Series Sheets by CMT Method, The International Journal of Materials and Engineering Technology (TIJMET), **2023**, 6(2):59-65

thickness of 1.5 mm. ER4043 (AlSi5) was used as filler wire. Chemical properties of the materials used are shown in Table 1, and mechanical properties are shown in Table 2.

Table 1. Chemical properties of the materials used (%)

Material	Fe	C	Si	Mn	Zn	Ti	Al
DP800	97	0,15	0,46	1,65	0,02	0,01	0,03
AL5182	0,19	-	0,10	0,37	0,01	0,02	99
ER4043	0,5	-	5	0,03	-	0,01	94

Table 2. Mechanical properties of test specimens and filler wire

Material	Yield stresses (σAk)	Tensile strength (σmax)	Elongation (%)	Hardness (Hv)
DP800	620 MPa	830 MPa	15	220
AL5182	160 MPa	282 MPa	23	-
ER4043	115 MPa	145 MPa	15	-

2.2. Method applied

The joints were made by CMT-joining method with ER4043 (AlSi5) filler wire with a diameter of 1 mm. Test specimens were cut and prepared 250x200 mm. 100% Argon shielding gas was used in the joints. Fully automatic mode was used in ABB IRB1600 robotic system for the applications. A special apparatus suitable for the lap joint position was made and integrated into the robotic system. Al-Steel plates joined at different current (75A, 80A, 85A, 90A, 95A, 100A, 105A, 110A) were prepared using laser cutting and tensile tests were performed on a ZwickRoell Z100 device according to the ISO 6892-1:2001 standard, tensile test specimen example is shown in figure 2. Bending tests were carried out by 3-axis bending method with Instron UTM-HYD 300DX device with 300 kN capacity according to TSE EN ISO 5173:2010/A1 standard. The hardness values of the specimens were taken by using the Vickers method according to EN ISO 6507 standard with a 100 g load vr pyramid pricking tip. For each method, 3 specimens were tested. For macro and micro imaging, the samples were sanded, polished and etched using 3% Nital (3 mL HNO3 and 97 mL H2O) reagents for 8 seconds. A 500x optical microscope and a JOEL JSM-6060LV scanning electron microscope (SEM) were used for imaging. Table 3 shows the applied welding parameters. Figure 2 shows the welding machine and test fixture.

2.3. Combining method with CMT

Joints were made using the cold metal transfer (CMT) MIG/MAG process with the new generation TPSi400 welding machine developed by Fronius international gmbh. Figure 3. shows the application logic of the cold metal transfer method and the formation of the arc according to Ampere/Voltage.

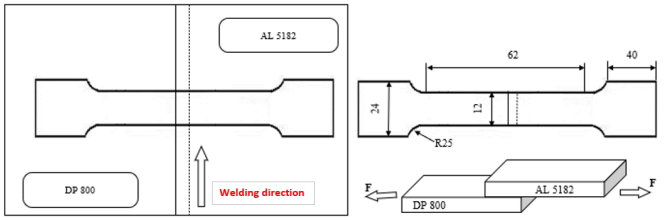

Figure 1. Tensile test specimen example

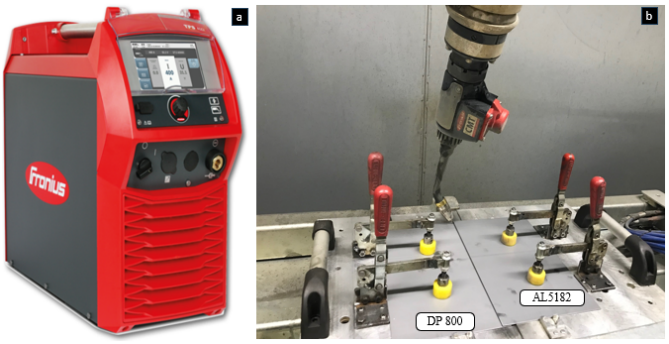

Figure 2. CMT welding machine (a), fixture, specimen and position (b)

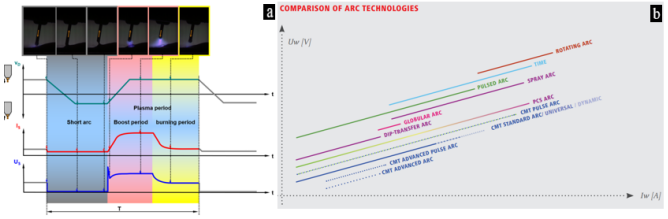

Figure 3. CMT application logic (a), Ampere/Voltage effect table of welding arcs (b) [12]

3. Results and discussion

3.1. Heat inputs and tensile test results

As a result of joining 1 mm DP800 galvanized steel plates and AL5182 plates in the overlap position using ER4043 (AlSi5) filler wire, the maximum strength values measured for each connection are shown in Figure 4(b). The maximum strength value of 4.28 kN was measured in the specimen joined with 90 amperes. The failure zones of the specimens welded at different amperages after tensile test are shown in Figure 4 (a).

Table 3. CMT- Joining parameters.

Material (Sample)	Welding Current(A)	Voltage (V)	Processing speed(cm/min)	Wire feed rate (m/min)	Protective gas flow rate(L/min)	Torch angle (^{0})
N-1	75	11,3	70	6,1	15	75
N-2	80	11,6	70	6,3	15	75
N-3	85	11,9	70	6,4	15	75
N-4	90	12,1	70	7	15	75
N-5	95	12,4	70	7,5	15	75
N-6	100	12,6	70	7,7	15	75
N-7	105	12,8	70	8	15	75
N-8	110	13,1	70	8,2	15	75

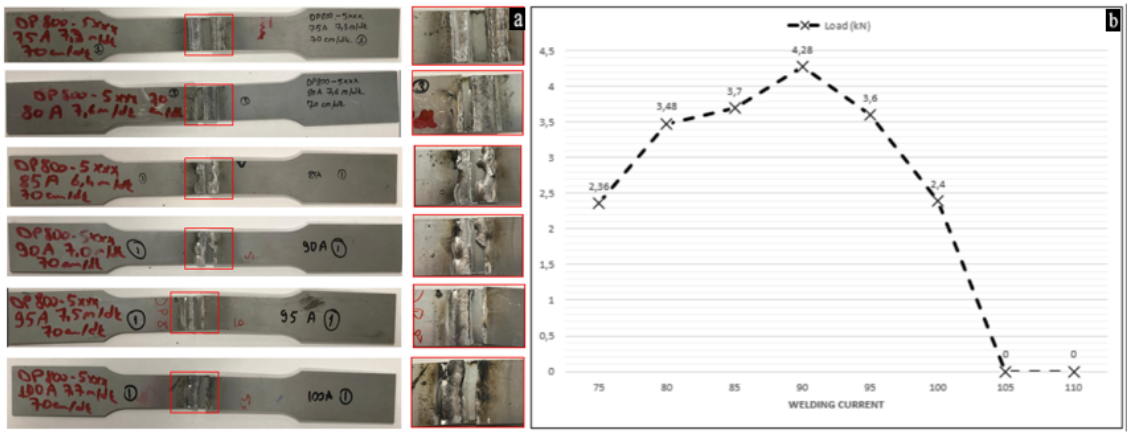

Figure 4. Tensile specimens and failure zones (a), graph of failure strength values (b)

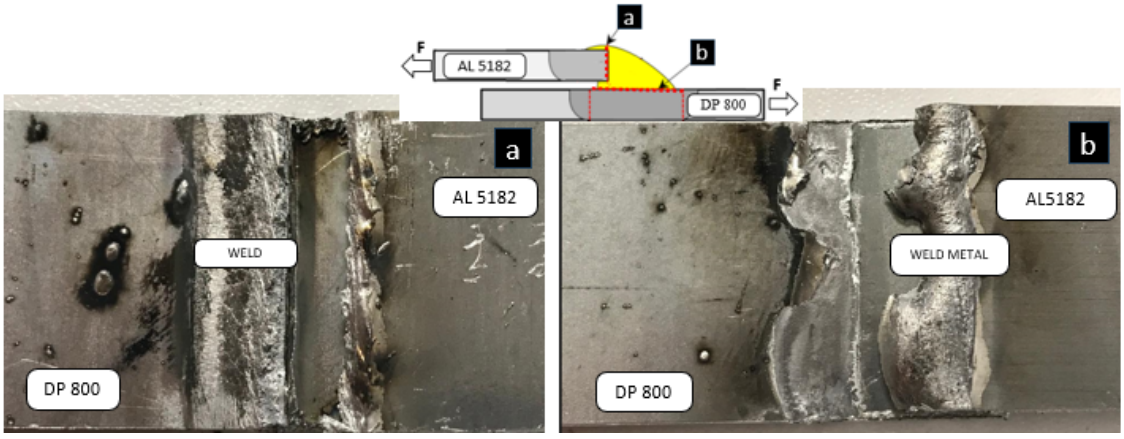

Figure 5. Failure near the heat affected zone (a), failure near the IMC layer (b)

In this research, the fracture location of the tensile test specimens was investigated in two different ways: (a) aluminum fracture is a type of fracture that occurs from the root of the weld seam towards the HAZ (Heat Affected Zone) due to incomplete melting or porosity in the weld root zone, as shown in Figure 5. coarsening grains and dissolution of different precipitates due to thermal cycling make this region weaker. (b) brazed interfaces inter metallic compound (IMC) fracture is the fracture stress occurring at the interface of steel and aluminum. These results can be explained by the thickness of the IMC layer. In another saying, the fracture varies with the variation of amperage and heat input.

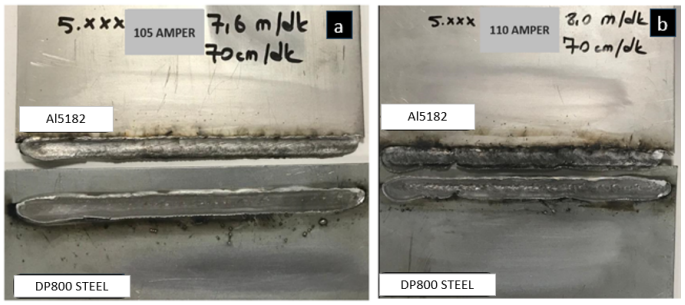

Figure 6. N-7(a) and N-8(b) failed joint test specimens

In Figure 6, the connections with N-7 (105 A) and N-8 (110 A) could not be obtained and therefore test values could not be obtained. It is observed that the thickness of the intermetallic structure increases with increasing heat input, which is known to negatively affect the bonding. In line with this information, it is thought that increasing heat input increases the thickness of the intermetallic structure above the threshold value and fusion cannot be achieved.

The variation of the welding current shown in Figure 7 is a factor in determining its effect on the tensile strength. Differences in tensile strength test results of connections made with different amperage values may be reflected by different levels of thickness of the IMC layer. It can be said that the increase in IMC layer thickness varies with the change of welding current. It is seen that this increase negatively affects the fracturing strength.

The heat inputs for the joints were calculated with the following formula (1), it was observed that the heat input increased in the joints at constant speed with the welding current and voltage increases.

Heat input formula;

$$Q\left(\frac{j}{mm}\right) = \frac{I(A)xU(V)x60}{V\left(\frac{mm}{dk}\right)} \quad (1)$$

Q = Heat input (J/mm), U = Voltage (V), v = Processing speed(cm/min), I = Welding Current (A),

Based on the results outlined in Figure 8 and Figure 7, heat input, amperage, IMC layer was found to be significant factors in determining the strength and fracture of joints. As the heat input increases, the tensile strength decreases as the grain sizes in the region where the HAZ is located change in the direction of increase. In short, an optimal amperage value was formed to achieve the highest tensile strength, the high heat input caused the tensile strength to decrease, resulting in a thicker, brittle IMC layer.

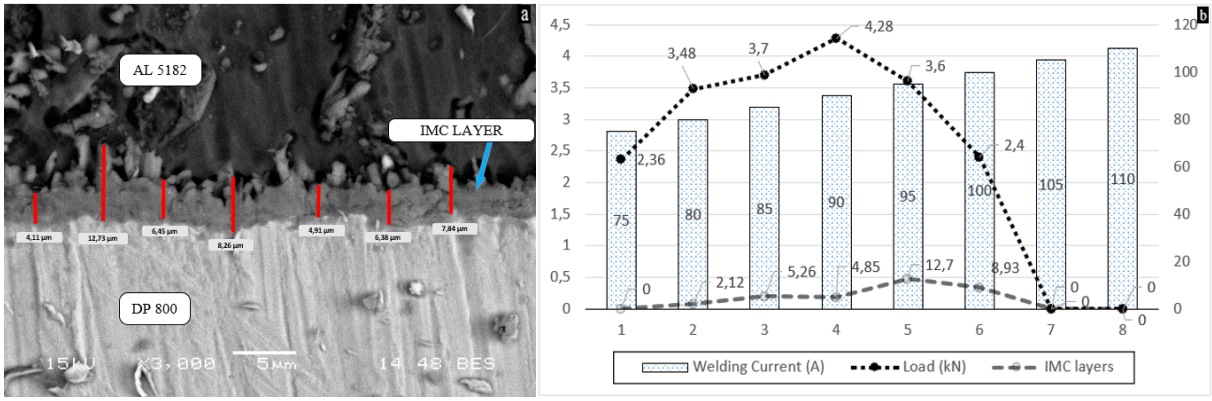

Figure 7. Variable values of IMC thicknesses of N-4 (a), amperage, IMC, load (kN) graph of joints (b)

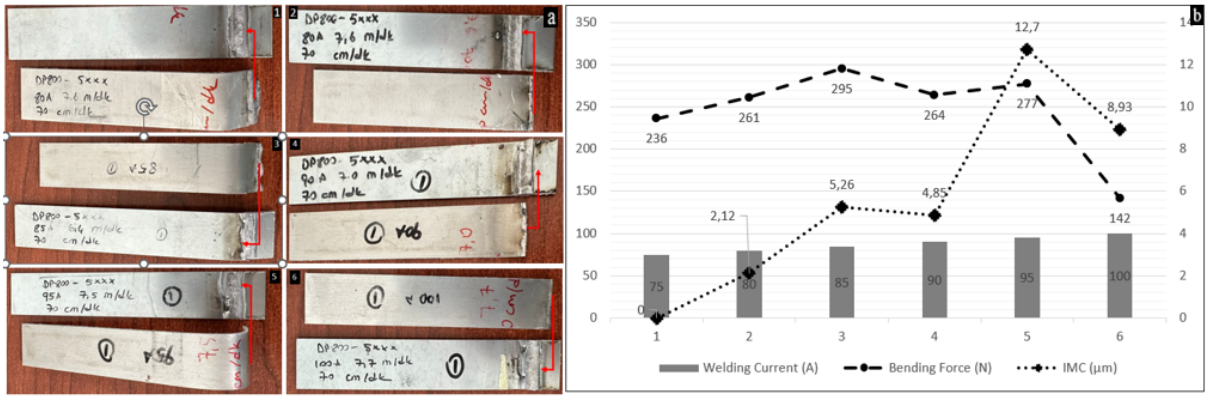

Figure 9. Images of flexure test results (a), welding current, bending force, IMC layer comparison graph (b)

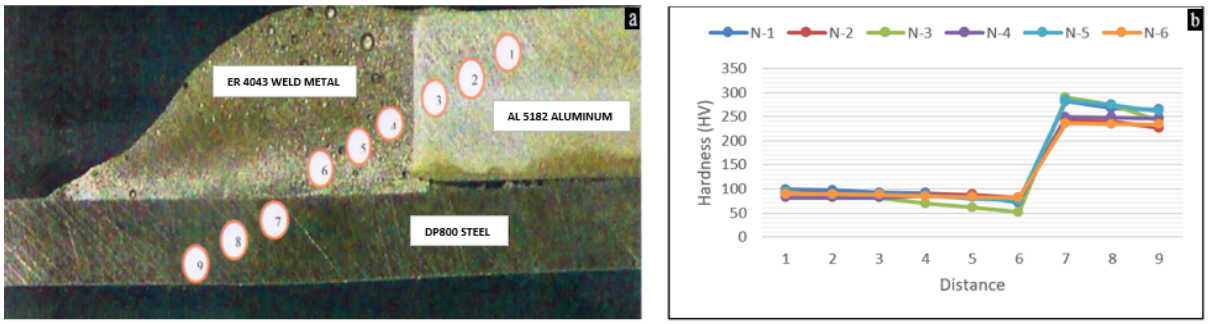

Figure 10. Hardness (Hv) points of lap joint (a), comparison graph of hardness (Hv) values (b)

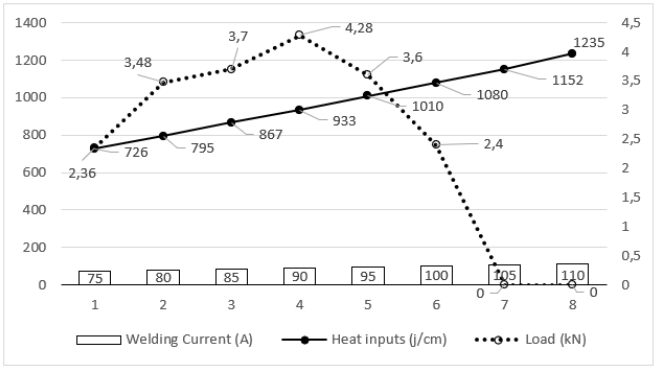

Figure 8. Welding current (A), load (kN), heat input graph of the joints

3.2. Bending test results

The results of the flexure test of the joined specimens are given in Table 4 and Figure 9.

Figure 9. shows that the highest fracture force (295 N) was reached at 85 (A) at N-3 and the lowest fracture force (142 N) was reached at 100 (A) at N-6. IMC thicknesses varied in these tests, supporting that this variation affects the mechanical properties. In addition, the amount of porosity formed in the weld seam is high and these porosities are a factor in the formation of important crack initiation zones.

Table 4. Bending test data of assembled samples

Definition (Sample)	Welding current (A)	Heat input (j/mm)	F_m(kN)	IMC (µm)	Bending Force (N)
N-1	75	726	2,36	1,11	236
N-2	80	795	3,48	2,12	261
N-3	85	867	3,7	5,26	295
N-4	90	933	4,28	4,85	264
N-5	95	1010	3,6	12,7	277
N-6	100	1080	2,4	8,93	142

3.3. Hardness test results

Hardness values taken from the samples are given in Table 5. A total of 9 measurements were taken on the weld metal and the hardness distribution curve in the transition zones was created.

Table 5. Hardness (Hv) values at reference points

Definition	1	2	3	4	5	6	7	8	9
N-1	98,6	97,3	92	91,4	85,9	71,3	282	268	264
N-2	94,7	89,1	85,4	89,3	88,3	81,4	243	240	226
N-3	94,1	84,2	81,5	68,9	62,1	51,1	290	274	242
N-4	81,4	81,1	80,8	86,4	84,8	74,1	250	248	247
N-5	91,2	88,8	88,5	85,9	80,2	76,6	284	274	261
N-6	89	88,9	88,4	84,6	82,6	80,9	236	235	233

The hardness points of the lap joint specimens and the comparison of the specimens with each other at these points are shown in Figure 10. With the formation of intermetallic layers of different thicknesses, it was found that the layer, which was soft in the region close to aluminum, was harder in the regions closer to steel.

It is known that as the pores formed in the chemical composition and the weld metal of the IMC structure differ, the hardness values will also change.

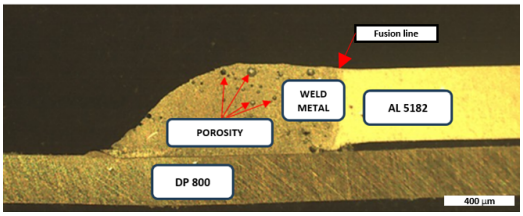

Figure 11. Joining zone failures

Figure 11 shows that porosities are formed in the weld joint as you move towards aluminum. It is estimated that the formation of porosity may be caused by shielding gas or zinc vapor that may be trapped in the weld pool. Zhang et al. concluded that zinc from the steel coating dissolves in the filler metal at the steel-aluminum interface after the joint and some of it evaporates and causes porosity in the weld seam [13].

3.4. Investigation of macro structures

During CMT welding of aluminum to steel, it is known that the zinc vapor remaining in the weld zone and the silicon content in the filler metal affect the wetting capacity of the filler metal [15]. The molten zinc and molten aluminum not only affected and reduced the surface tension of the molten aluminum, but also released the mixing energy in the fusion zone, causing the filler wire to spread [14]. As shown in Figure 12, the weld seam width was measured as 4.48 mm in specimen 4 and the highest breaking strength was determined as 4.28 kN. As the weld width changes, the breaking strength also changes.

3.5. Investigation of micro structures

Examining the microstructures and intermetallic layers shows that the effect of heat input during the MIG welding-fusion process affects the average thickness of the IMC layer formed between the steel and the fusion zone. It has been observed that the thickness of the IMC layer changes with the change in welding current. For example, in Figure 13, the average thickness of the IMC layer for the 95 (A) welded specimen was about 12.7 µm, while for the 75 (A) welded specimen it was about 1.1 µm.

Since the cooling rate during MIG welding-hard brazing varied in different regions, it formed an IMC layer of different thickness. Depending on the chemical composition and amperage of the filler wire, IMC layer thickness is different, and according to the results mentioned above, the thickness of the IMC layer varies not only with the filler wire but also with changing the heat input. This affected the mechanical properties of the welds between the welded specimens. Alloy ratios (%) of the joint areas shows in Table 6.

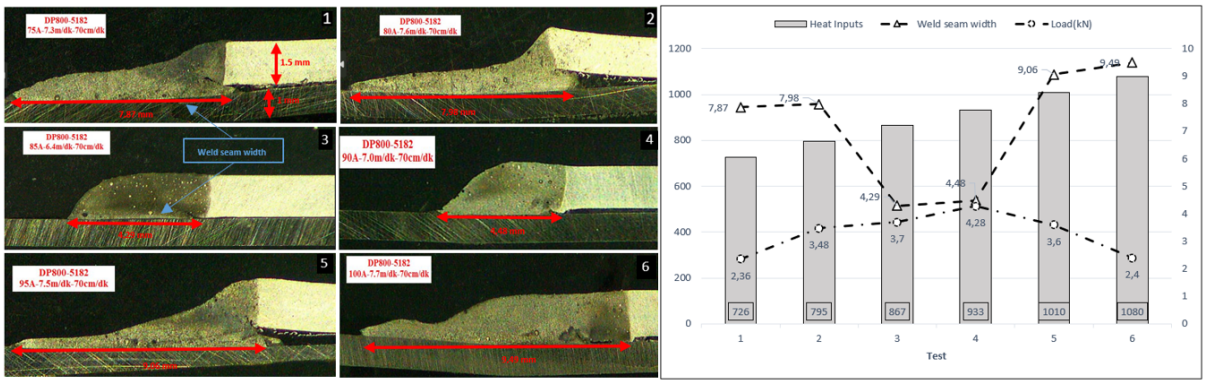

Figure 12. Sample-1-2-3-4-5-6 macro images and head inputs, load, weld seam width comparison

The alloy values determined in Figure 15 are taken from the reference points in Figure 14. Considering the wt.% ratio, it is seen from the phase diagram according to the wt.% ratio of metals that the IMC type is the intermetallic phase for all samples. Differences were observed in the wt% ratios of aluminum and iron obtained in the EDS results, and the brittle phases Fe3Al, FeAl2, FeAl3 and Fe2Al5, brittle phases predicted to form at the interface appear in the IMC layer. It should be noted that at low welding currents (85 A) where the amount of heat input is very low, the variation in thickness of the IMC layer does not follow a certain rule. The reason for this behavior may be due to the low heat input generated at low welding currents. That is, at low heat input, Si could not affect and control the thickness of the IMC layer. Maybe this is because Si cannot increase the solubility of Fe in molten aluminum and therefore cannot control the thickness of the IMC layer, the fluctuations in the IMC thickness are too high and the indentations are too large. Zhang and others. It has been reported that the intermetallic layer formed between the weld metal and the steel extends into the weld metal in sawtooth shape at low heat input, this layer penetrates the weld metal (tongue-like) and is thicker at higher heat input. values [17-19].

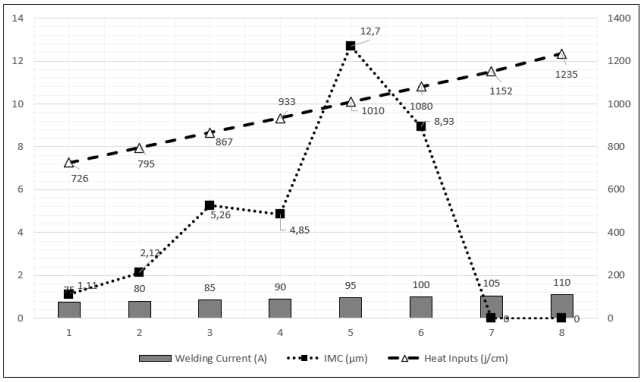

Figure 13. Comparison graph of heat inputs, welding current, IMC of the joints

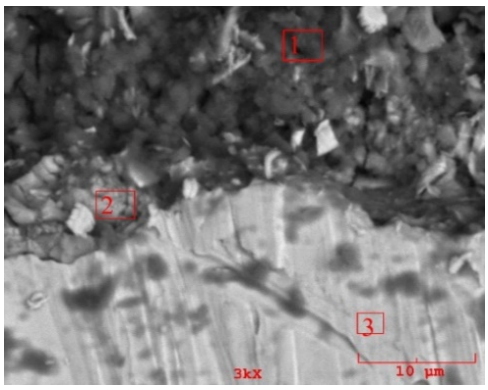

Figure 14. SEM-EDS analysis points of the sample

Table 6. Alloy ratios (%) of the joint areas.

W. Current	Definition	C	Mg	Al	Si	Ti	Mn	Fe	Zn
75	N-1.1	8,649	4,430	36,783	3,720	0,545	2,004	36,059	7,809
	N-1.2	0,617	0,854	23,314	2,493	0,678	1,616	62,220	8,207
	N-1.3	0,193	0,694	1,419	1,586	0,012	1,518	93,337	1,242
80	N-2.1	0.000	0,690	96,935	0,732	0,037	0,334	0,302	0,971
	N-2.2	0,655	1,114	45,571	2,897	0,359	0,310	46,009	3,085
	N-2.3	0,011	0,105	0,908	1,286	0,218	1,893	94,050	1,539
85	N-3.1	0,481	0,558	65,374	29,092	0,105	0,294	2,177	1,918
	N-3.2	0.000	0,300	53,264	3,542	0,019	0,785	41,147	0,943
	N-3.3	0,123	0,097	1,285	2,008	0,180	1,752	93,235	1,443
90	N-4.1	0.000	0,525	92,624	3,034	0,177	0,762	2,616	0,264
	N-4.2	0.000	0,126	61,843	5,670	0,124	0,736	29,647	1,855
	N-4.3	0,118	0,374	0,861	1,380	0,090	2,219	93,938	1,138
95	N-5.1	0,545	1,140	45,010	3,655	0,193	0,592	44,907	3,959
	N-5.2	0.000	0,188	50,370	2,535	0,142	0,889	44,325	1,552
	N-5.3	0,131	0,270	1,850	1,542	0,172	1,427	93,007	1,731
100	N-6.1	0.000	1,190	86,880	2,854	0,481	0,596	3,378	4,622
	N-6.2	0.000	0,230	45,349	5,874	0,244	0,526	43,156	4,621
	N-6.3	0,120	0,126	0,294	0,910	0,155	1,366	96,548	0,600

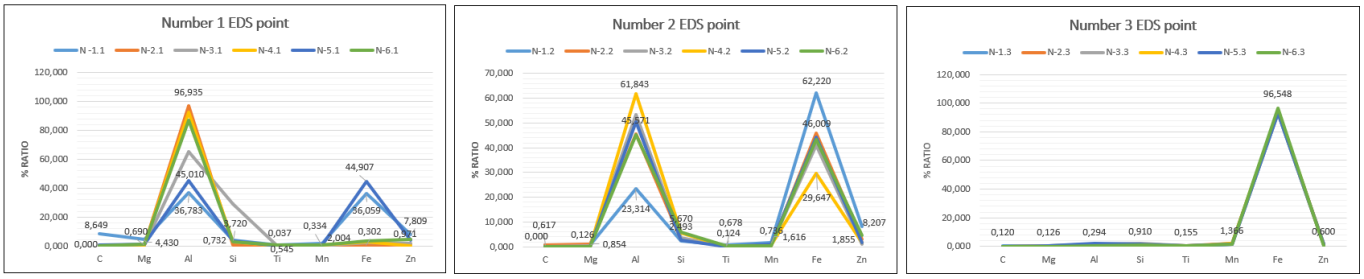

Figure 15. Alloy ratio chart for points 1/2/3 (%)

4. Conclusions

The maximum breaking strength value in the joints was 4.28 kN in the sample joined with 90 A. Fm: 4.28 kN and the breaking strength of the joints at different amperage values varies.

It was determined that intermetallic (IMC) phase formation was observed between the joined aluminum and steel samples and the thickness of this phase changed with the heat input.

After joining, it was determined that the highest fracture force (295 N) value in bending tests was reached at the lowest IMC thickness, and the fracture force was negatively affected as the IMC thickness increased.

The negative effects of evaporating galvanizing were observed in the Al-DP steel joints (incomplete melting, porosity formation). It was also observed that melting aluminum positively affects the wetting angle on galvanizing and directly affects the weld seam of the joints.

Acknowledgments

Ak-Pres Automotive A.Ş. and Sakarya University of Applied Sciences University Prof. Dr. Salim Aslanlar thank you for your support.

Author contributions

Cihan Yakupoğlu: Supervision, resources, roles/writing - original draft, writing - review & editing

Ufuk Öztürk: Data curation, formal analysis, conceptualization

İbrahim Acar: Investigation, methodology, resources

Faruk Varol: project administration, validation

References

1. Schierl, A., The CMT process a revolution in welding technology, Weld. World. **2005**
2. Shi, Y., Zhang, G., Huang, Y., Lu, L., Huang, J., Shao, Y., Pulsed double electrode GMAW brazing for joining of aluminum to steel, Weld. J. **2014**
3. Shao, L., Shi, Y., Huang, J., Wu, S., Effect of joining parameters on microstructure of dissimilar metal joints between aluminum and galvanized steel, Mater. Des. **2015**, 66, 453–458
4. Peyre, P., Sierra, G., Deschaux-Beaume, F., Stuart, D., Fras, G., Generation of aluminium–steel joints with laser-induced reactive wetting, Mater. Sci. Eng. **2007**, 444(1-2): 327–338
5. Park, H.J., Rhee, S., Kang, M.J., Kim, D.C., Joining of steel to aluminum alloy by AC pulse MIG welding, Mater. Trans. **2009**, 50(9):2314–2317
6. Boumerzoug Z., et al. Fabrication and welding of aluminum composite, The International Journal of Materials and Engineering Technology, **2022**, 5(2):71-74
7. Iwase, T., et al., Dissimilar metal joining between aluminum alloy and hot-dip aluminized steel sheet, Kobelco Technol. Rev. **2008**:29–34
8. Türkoğlu, R., Aydın, L., & Gültürk, E., Modelıng and Optımum Parameters of CO_2 Laser Mıg Hybrıd Weldıng Proces. The International Journal of Materials and Engineering Technology, **2021**, 4(2), 91-100
9. Babu, S., Panigrahi, S.K., Ram, G.J., Venkitakrishnan, P.V., Kumar, R.S., Cold metal transfer welding of aluminium alloy AA 2219 to austenitic stainless steel AISI 321. Journal of Materials Processing Technology, **2019**, 266:155-164
10. Madhavan, S., Kamaraj M., Vijayaraghavan, L., Microstructure and mechanical properties of cold metal transfer welded aluminium/dual phase steel, Science and Technology of Welding and Joining, **2016**, 21(3):194-200
11. Singh, J., Arora, K. S., & Shukla, D. K., Lap weld-brazing of aluminium to steel using novel cold metal transfer process, Journal of Materials Processing Technology, **2020**, 283, 116728
12. <https://www.fronius.com/tr-tr/turkey > Dated 11.06.2023
13. Zhang, H., T., Feng, J., C., He, P., Zhang, B.B., Chen, J.M., Wang, L., The Arc Characteristics and Metal Transfer Behaviour of Cold Metal Transfer and Its Use in Joining Aluminium to Zinc-Coated Steel, Materials Science and Engineering. **2009**, 499, 111-113
14. Yagati, K.P., Bathe, R.N., Rajulapati, K.V., Rao, K.B.S., Padmanabham, G., Fluxless arc weld-brazing of aluminium alloy to steel. Journal of Materials Processing Technology, **2014**, 214(12):2949-2959
15. Medgyesi, T., Popescu, M., Opris, C., Difficulties Encountered in Performing Dissimilar Joints On Sheets, Proceedings of The 22nd International DAAAM Symposium, Vienna, Austria, **2011**
16. Gullino, A, Matteis, P, D'Aiuto, F., Review of Aluminum-To-Steel Welding Technologies for Car-Body Applications. Metals; **2019**, 9(3): 315.
17. Dong, H., Hu, W., Duan, Y., Wang, X., Dong, C., Dissimilar metal joining of aluminum alloy to galvanized steel with Al–Si, Al–Cu, Al–Si–Cu and Zn–Al filler wires. J. Mater. Process. Technol. **2012**, 212, 458–464
18. Su, Y., Hua, X., Wu, Y., Influence of alloy elements on microstructure and mechanical property of aluminum–steel lap joint made by gas metal arc welding, J. Mater. Process. Technol, **2014**, 214, 750–755
19. Kobayashi, S., Yakou, T., Control of intermetallic compound layers at interface between steel and aluminum by diffusion-treatment [J]. Materials Science & Engineering A, **2002**, 338(1-2):44-53